J Porous Mater (2015) 22:621–628
DOI 10.1007/s10934-015-9934-8

Synthesis of silica aerogel microspheres by a two-step acid–base sol–gel reaction with emulsification technique

Yuxi Yu[1] · Deqian Guo[1] · Jiyu Fang[2]

Published online: 8 March 2015

Abstract Silica aerogel microspheres were synthesized by a two-step acid–base sol–gel reaction in water-in-oil emulsion systems, in which tetraethoxysilane was used as a precursor and ethanol as a solvent, and HCl and NH_4OH as acid–base catalysts in two steps. The synthesis process and parameters of the emulsion process including viscosity, surfactant concentration and stirring rate have been investigated. In the emulsifying process, the viscosity of silica sol is vital to restrain the occurrence of flocculation phenomenon for forming monodisperse alcogel microspheres. The smooth silica aerogel microspheres can be formed from the silica sol with the viscosity of 107 mPa s. The resultant silica aerogel microspheres with similar surface areas above 650 m^2/g, bulk densities in the range of 0.094–0.138 g/cm^3, and mean diameters ranging from 40.3 to 126.1 μm can be formed by controlling these parameters of the emulsion process. The minimum of polydispersity and roundness of silica aerogel microspheres are 0.058 and 1.11, respectively. Furthermore, silica aerogel microspheres show a high capacity of uptaking bean oil, isopropanol, kerosene and *n*-hexane, highlighting the possibility to remove oils from water for oil spill cleanup.

✉ Yuxi Yu
yu_heart@xmu.edu.cn

✉ Jiyu Fang
jfang@mail.ucf.edu

[1] Department of Materials Science and Engineering, College of Materials, Xiamen University, Xiamen 361005, China

[2] Department of Materials Science and Engineering, Materials Processing and Analysis Center, University of Central Florida, Orlando, FL 32816, USA

Keywords Silica aerogel microspheres · Water-in-oil emulsion · Organic solvent uptaking · Porous materials

1 Introduction

Aerogels are an extremely porous and ultralight material. They have large internal surface area, low thermal conductivity, low optical refractive index, and low permittivity [1–6]. In recent years, there has been interesting in exploiting the potential application of aerogels for thermal insulation [7, 8], energy storage [9–12], electrochemical process [13, 14], drug delivery [15], waste water treatment [16], organic liquid adsorption [17], and oil clean-up [18, 19].

Silica aerogel microspheres are attractive due to their low friction coefficients, good fluidities, and uniform stress–strain behaviors. They also show promise as delivery systems for the controlled release of drugs [20] and tire elastomers [21]. Generally speaking, silica aerogels are brittle materials. The powder from mechanically milled silica aerogel monoliths often has irregular shapes and poor liquidities. It is also a challenge of using micro-fabrication technologies to produce spherical silica aerogels. Recently, some progresses have been made for forming silica aerogel microspheres by water/oil (W/O) emulsion methods [20, 22, 23]. Although it is feasible to form sol droplets in the continuous phase under strong agitations, the droplets easily flocculate to form flocs.

In this paper, we synthesized silica aerogel microspheres through a two-step acid–base sol–gel reaction in W/O emulsions. We find that the viscosity of silica sol is a key for the formation of smooth silica aerogel microspheres. The size of smooth silica aerogel microspheres can be changed by altering silica sol viscosities, surfactant concentrations, and mechanical stirring rates. Furthermore, we

exploited the application of smooth silica aerogel microspheres for the absorption of different organic solvents.

2 Experimental section

2.1 Reagents

Tetraethoxysilane (TEOS), isopropanol, kerosene, *n*-hexane and ethanol (EtOH) with a purity of 99 % were purchased from Sinopharm Chemical Reagent Co. Ltd. Deionized water (H_2O) was prepared by an ion exchange system (18 MΩ and pH 5.7). Alkylphenol ethoxylate (surfactant), hydrochloric acid (HCl) and ammonia water (NH_4OH) were purchased from Xilong Chemcial Co. Ltd. Bean oil was purchased from supermarket of Shopping Time. All chemicals were used without further purification.

2.2 Characterization methods

The pH value of silica sol was measured by a Merttler pH meter (FE-20, Mettler Toledo, Zurich, Switzerland). The viscosity of silica sol was measured by a viscometer (NDJ-8S, Fangrui Instrument CO., LTD, Shanghai, China). The bulk density ($\rho = m/V$) of silica aerogel microspheres was calculated based on their mass (m) to volume (v) ratios. The volume was analyzed by a measuring cylinder, and the mass was measured by an electronic microbalance with an accuracy of 10^{-5} mg. The textural properties of silica aerogel microspheres were investigated by the standard gas adsorption method using surface area analyzer (TtiStar II, Micromeritics, USA). The surface area of silica aerogel microspheres was calculated by using the Brunauer Emmett and Teller (BET) method at various partial pressures ($0.01 < p/p_0 < 1$). The pore size distributions of silica aerogel microspheres were measured by using the Barrette Joyner Halenda (BJH) method. The microstructure of silica aerogel microspheres was characterized by scanning electron microscopy (SEM, TM-3000, Hitachi High-Tech, Tokyo, Japan). The roundness of silica aerogel microspheres was defined as a semi-major axis/semi-minor axis ratio. Thermo gravimetric analysis (TGA/DTA, STA 409 EP/DIL 404, Netzsch, Selb, Germany) was conducted from room temperature to 1200 °C with a rate of 10 °C/min under air flow. The chemical structure of silica aerogel microspheres was characterized by Fourier transform-infrared spectroscopy (FT-IR, Avatar 360, Thermo Nicolet, Madison, USA).

2.3 Synthesis of silica aerogel microspheres

Figure 1 shows a schematic representation of the formation of silica aerogel microspheres. The experimental process consists of three basic steps: (1) The preparation of W/O emulsion. EtOH, H_2O, and TEOS were placed into a boiling flask and then stirred for 30 min by a mechanical stirrer at room temperature, followed by the addition of EtOH diluted hydrochloric acid solution and ammonia water to form silica sol. The molar ratio of the mixture is 1 mol TEOS: 8 mol EtOH: 3 mol H_2O: 6.0×10^{-5} mol HCl: 1.0×10^{-2} mol NH_4OH. The gel time of silica sol was approximate 90 min. W/O emulsion was obtained by pouring silica sol into the continuous phase composed of soybean oil and alkylphenol ethoxylate under high-speed mechanical agitation. (2) The formation of silica alcogel microspheres. The mechanical agitation was stopped after the sol-to-gel transition for the creaming of emulsions. The silica alcogel microspheres were separated with a separatory funnel and washed for several times with EtOH, followed by aging in an EtOH bath for 12 h. (3) EtOH supercritical drying. Silica alcogel microspheres were EtOH supercritical dried at 260 °C with a electrical band heater, meanwhile the desired working pressure (11.0–13.0 MPa) was reached [24, 25].

3 Results and discussion

3.1 Synthesis process

In the formation process of silica alcogel microspheres, silica sol droplets could either directly translate into silica alcogel microspheres or undergo grain growth or flocculation before the translation as shown in Fig. 1. Although W/O emulsion maintains a certain stability under strong agitation, silica sol droplets suffer from unequally shear forces under high-speed stirring. The large silica sol droplets are liable to ascent and flocculate to form flocs as the force exceeds their Brownian motion. It can be seen in Fig. 2, some small microspheres appear to aggregate, which is attributed to the reconstitution of flocs. So, it is vital to restrain the flocculation for the preparation of silica aerogel microspheres. However, the mechanism and process for 'the regular arrangement of three-dimensional ball need further exploration. During the sol-to-gel transition, as silica sol gradually becomes viscous and the flocs reunite to form big balls. After stopping mechanical stirring, the creaming of emulsion systems occured automatically due to the density difference between the two phases. The silica alcogel microspheres floated on the oil phase were washed repeatedly for wiping off the oil phase. Finally, silica aerogel microspheres were acquired after EtOH supercritical drying.

3.2 Effect of viscosities

In the sol-to-gel transition, silica sol gradually becomes viscous and finally turns into a gel. The speed of the

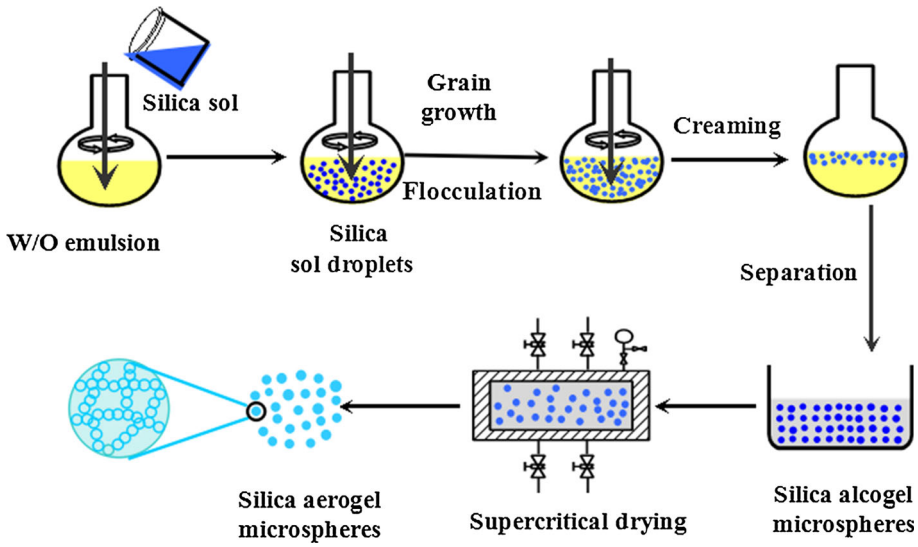

Fig. 1 Schematic representation of the formation of silica aerogel microspheres

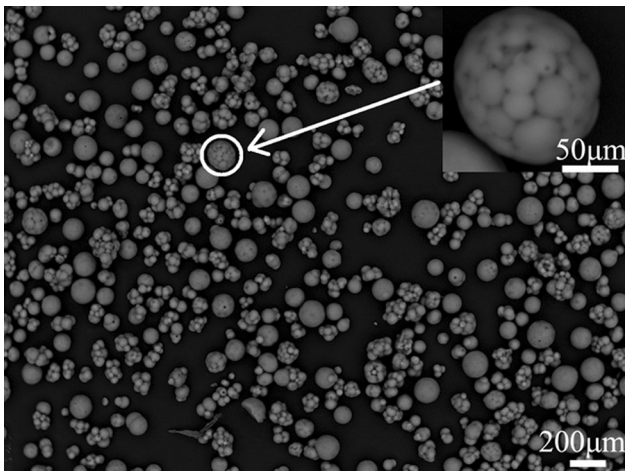

Fig. 2 SEM images of silica aerogel microspheres. (600 rpm, 0.3 % surfactant)

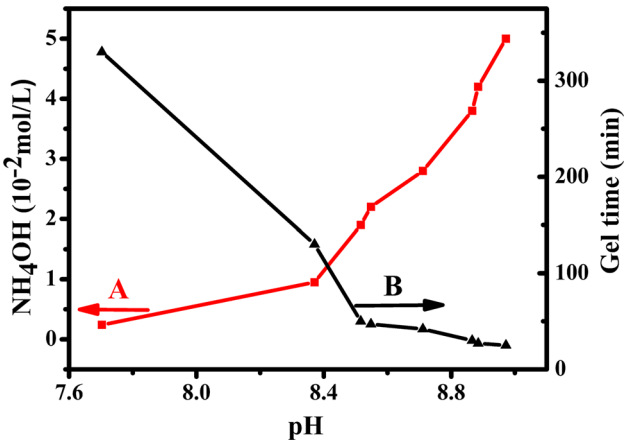

Fig. 3 The effect of NH_4OH concentrations on pH values and gel time of silica sol

transformation largely depends on NH_4OH concentrations (Fig. 3). The increase of NH_4OH concentrations leads to the increase of pH values of silica sol (curve A), which reduces the gel time (curve B). It has been shown that silica sol tends to form a three-dimensional porous silica network in the pH range from 6 to 8 [26]. Thus, silica sol was prepared at the pH of 8.36 in our experiments. We note that the viscosity of silica sol increases from 100 to 900 mPa s as the gel time changes from 50 to 90 min (Fig. 4). We note that the viscosity of silica sol slowly increases from 100 mPa s as the gel time increases from 50 to 70 min. Beyond 70 min, the viscosity of silica sol grows exponentially and reaches to 900 mPa s at 82 min. In the end, the entire system becomes a crosslinked network and becomes a silica alcogel.

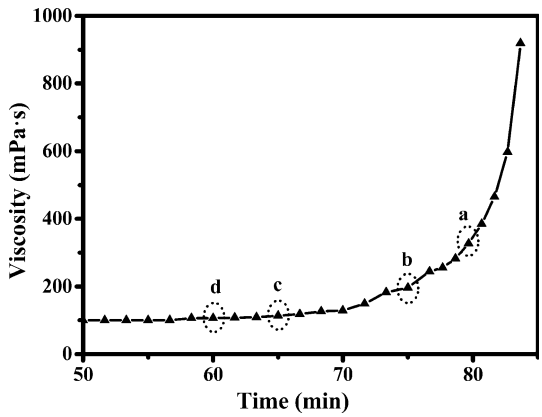

Fig. 4 Viscosity of silica sol as a function of time at 25 °C. *a* 80 min, 322 mPa s, *b* 75 min, 195 mPa s, *c* 70 min, 133 mPa s, and *d* 60 min, 107 mPa s

We optimize the viscosity of silica sol to achieve the control of the morphology of silica alcogel microspheres. It is a principal factor to restrain the flocculation for the preparation of silica aerogel microspheres. Figure 5 shows the morphologies of the silica aerogel microspheres formed at different viscosities by mixing two phases at different time. The silica aerogel microsphere in Fig. 5a was formed from the silica sol with the viscosity of 322 mPa s into the continuous phase. The silica sol droplets gelated rapidly before being enveloped steadily by the continuous phase due to the short sol–gel time. The alcogel microsphere shows a scraggly surface destroyed by the strong shear force. The silica aerogel microsphere in Fig. 5b, c was formed from the silica sol with the viscosity of 195 and 133 mPa s, respectively. The lower the viscosity of silica sol, the longer the sol–gel time. There are enough time for the continuous phase enveloping the silica sol droplets. As the mutation in viscosity, as the enveloped unsteadily silica sol droplets collide with each other, a few small droplets inserted into a big one and turned into a whole. When the viscosity of silica sol was reduced to 107 mPa s, the silica sol droplets were enveloped steadily by the continuous phase and then gelated, leading to the formation of a smooth surface. The enveloped droplets with a good sphericity were hard to flocculate, leading to tiny agglomeration. It is clear that the appropriate viscosity is critical for the formation of silica alcogel microspheres with a smooth and uniform surface.

3.3 Effect of surfactant concentrations

We study the effect of surfactant concentrations and stirring speeds on the formation of silica aerogel microspheres. Table 1 summarizes the bulk density, particle size, roundness, surface area, and pore volume of silica aerogel microspheres formed at different surfactant concentrations and stirring speeds. In the first set of experiments (S1–S4), alkylphenol ethoxylate with different concentrations was added into the continuous phase, while all other parameters were kept constant. We find that silica aerogel microspheres show the smallest diameter and roundness and the largest density and surface area at 0.6 wt% of alkylphenol ethoxylate (S2). The surface tension between the dispersed phase and the continuous phase depends on surfactant concentrations [27]. The reduction of the surface tension leads to the reduction of impetus of Oswald ripening. Besides, surfactants generate Gibbs elasticity which weakens the ability of grain growth. Therefore, there is an optimum surfactant concentration at which the formed silica aerogel microspheres have the smallest diameter and roundness.

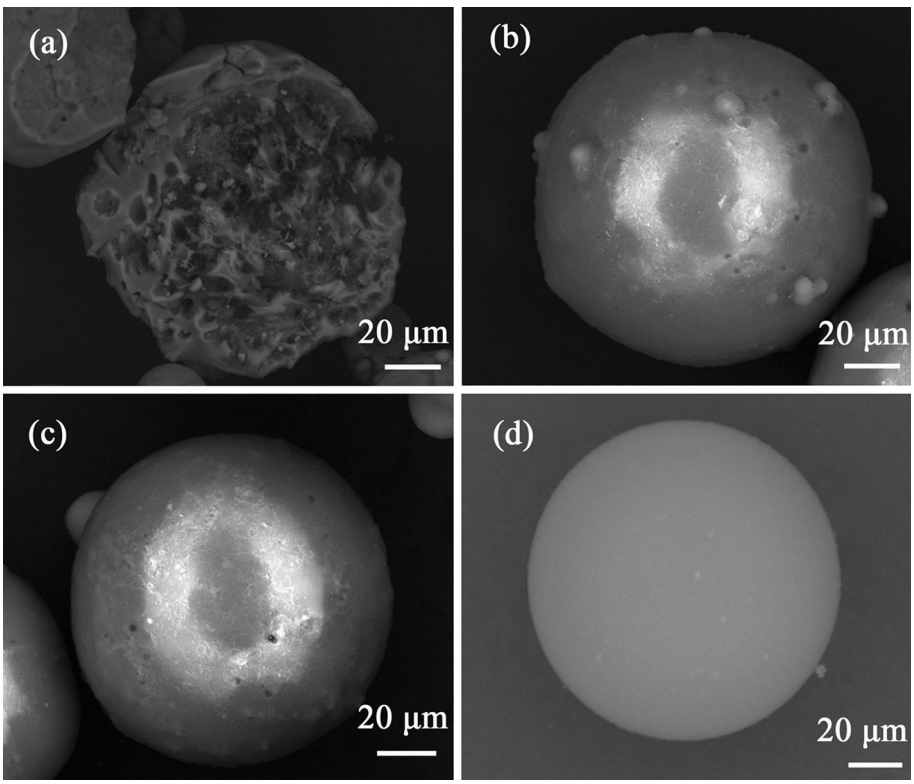

Fig. 5 SEM images of silica aerogel microspheres prepared by mixing two phases at different viscosities of silica sol: **a** 322 mPa s, **b** 195 mPa s, **c** 133 mPa s, and **d** 107 mPa s (600 rpm, 0.6 % surfactant)

Table 1 Physical properties of silica aerogel microspheres

Group No.	Surfactant (wt%)	Rotate speed (rpm)	Mesh sieves (mesh)	Bulk density (g/cm^3)	Particle size (μm)	Surface area (m^2/g)	Roundness
S1	0.3	800	100	0.116	117.4	661.0	1.32
S2	0.6	800	100	0.127	113.8	665.5	1.24
S3	1.2	800	100	0.111	120.5	651.3	1.30
S4	2.4	800	100	0.094	126.1	657.4	1.25
S5	0.6	600	300	0.100	45.5	755.5	1.18
S6	0.6	700	300	0.118	43.9	717.9	1.16
S7	0.6	800	300	0.122	42.9	703.4	1.14
S8	0.6	900	300	0.138	40.3	712.3	1.11

3.4 Effect of stirring speeds

In the second set of experiments (S5–S8), we varied the stirring speeds, while all other parameters were kept constant. The silica aerogel microspheres (S5–S8) are much smaller than those prepared in the first set of experiments (S1–S4), attributing to different physical screening. We find that the mean diameter of silica aerogel microspheres decreases from 45.5 to 40.3 μm by varying the stirring speeds from 600 to 900 rpm, while their roundness decreases from 1.18 to 1.11. The minimum and maximum polydispersity of silica aerogel microspheres are 0.058 (S5) and 0.071 (S8) [28]. The increase of stirring speeds results in more energy being input to the system to form form smaller sol droplets, which suppresses the creaming and flocculation and leads to the reduce of roundness. Figure 6 shows the morphology and diameter distribution of silica aerogel microspheres prepared at different stirring speeds. Obviously, the diameter of these microspheres with a smooth surface decreases with the increase of stirring speeds.

3.5 Structure and thermal properties

Figure 7 is the nitrogen adsorption–desorption isotherms of S5–S8 samples listed in Table 1. As stirring speed reduces, the sol–gel time of smaller silica sol droplets extends, the formed porous structure becomes more uniform distribution, the surface area of silica aerogel microspheres slightly increases. All the isotherms show typical IV absorptions. The N_2 gas adsorption occurs in the micropores at low pressures, followed by the adsorption in the mesopores, and capillary condensation at high pressures, leading to H_2-type hysteresis loops. At the process of capillary condensation, the adsorption quantity rises abruptly, resulting from narrow pore distributions. This suggests that silica aerogel microspheres have a character of aerogel structures with similar surface areas above 650 m^2/g. Informed by that, the stirring speed does not have effect on network structure of silica aerogels, the same as surfactant concentration and viscosity.

Figure 8 shows the FT-IR spectrum of silica aerogel microspheres (S5 sample). The peaks at 1080 and 454 cm^{-1} represent the stretching and bending of Si–O–Si groups, respectively. The peak at 797 cm^{-1} is related to the Si–O stretching and the peak at 3643 cm^{-1} is attributed to the stretching of Si–OH groups. The peaks at 2851 and 2948 cm^{-1} are related to the stretching of $–CH_3$ groups. This result proves that silica aerogel microspheres have $–CH_3$ terminal groups.

Figure 9 is the TG–DTA curve of silica aerogel microspheres (S5 sample), which shows that the total weight loss is approximate 9.9 %. In the temperature range from 25 to 100 °C, the weight declines 2.3 %, followed by 7.6 % of weight loss from 450 °C to 750 °C. Meanwhile the DTA curve shows the first endothermic peak at 100 °C, which is attributed to the volatilization of water and ethanol. It suggests that water and ethanol scarcely exist in silica aerogel microspheres. In the temperature range from 450 to 750 °C, the DTA curve shows the second exothermic peak at 500 °C, which is attributed to the decomposition of $–CH_3$ groups. The silica aerogel microspheres become hydrophilic.

3.6 Adsorption applications

Finally, we study the absorption property of the silica aerogel microspheres (S5 sample) in some solvents. The absorption ratio (Q) of silica aerogel microspheres is measured by Eq. 1. Where, m is the mass of silica aerogel microspheres, m_1 is the mass of silica aerogel microspheres screened with cloth after absorbing of solvents, and m_2 is the mass of the cloth after the absorption of solvents.

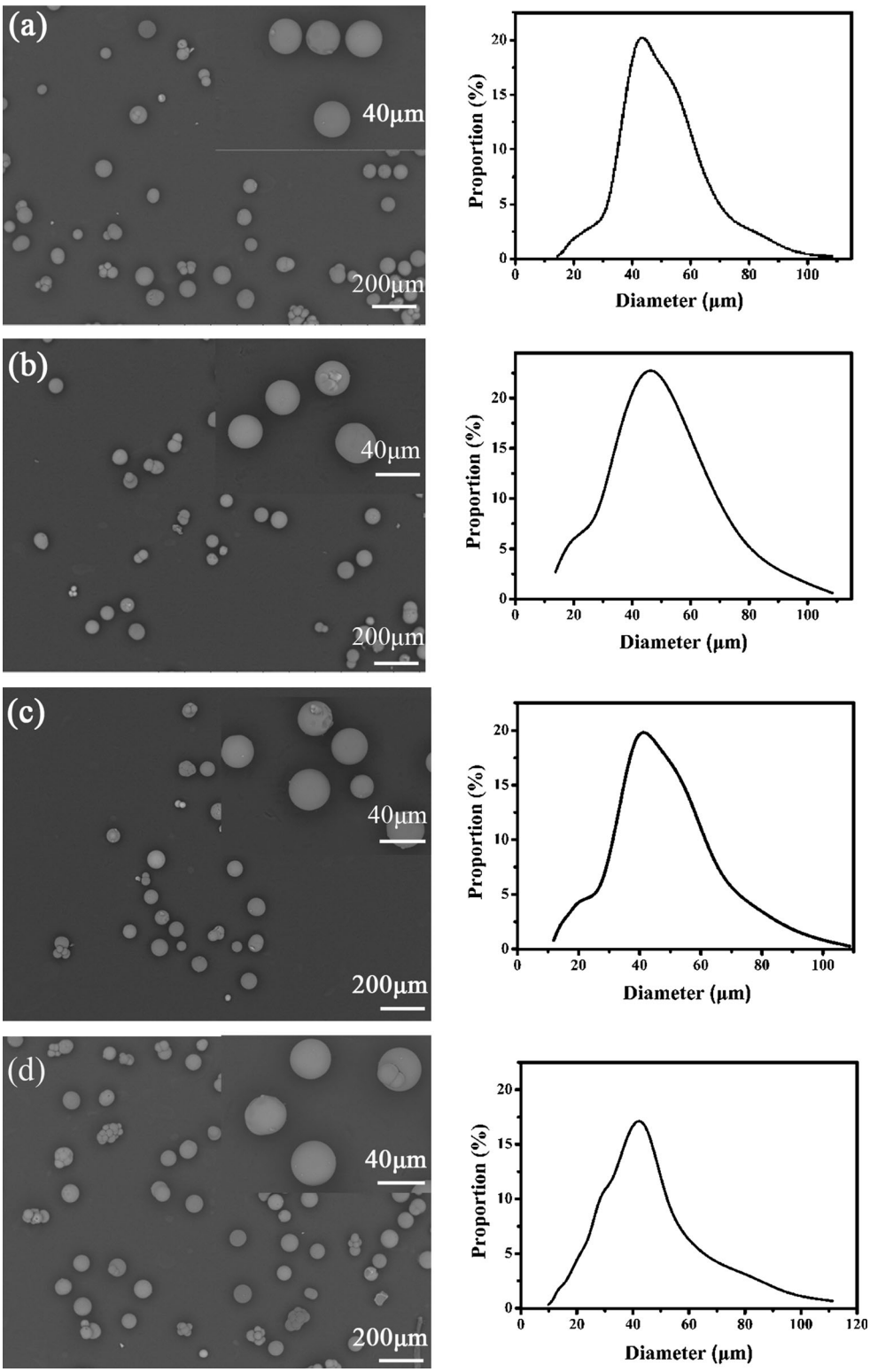

Fig. 6 SEM images and diameter distributions of silica aerogel microspheres formed at different stirring speeds: **a** 600 rpm, **b** 700 rpm, **c** 800 rpm, and **d** 900 rpm

$$Q = \frac{m1 - m2}{m} \quad (1)$$

Figure 10 gives the absorption ratios of silica aerogel microspheres for four solvents. It can be seen that silica aerogel microspheres without treating and 500 °C heated silica aerogel microspheres both show a high uptake capacity due to their hydrophobic porous structures. The absorption ratio is ~1019 % for bean oil, ~816 % for

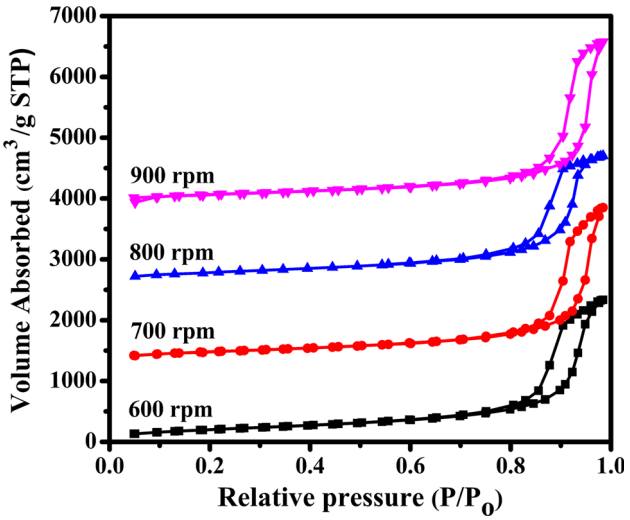

Fig. 7 Nitrogen adsorption–desorption isotherms of 150 °C-dried silica aerogel microspheres prepared at different stirring speeds

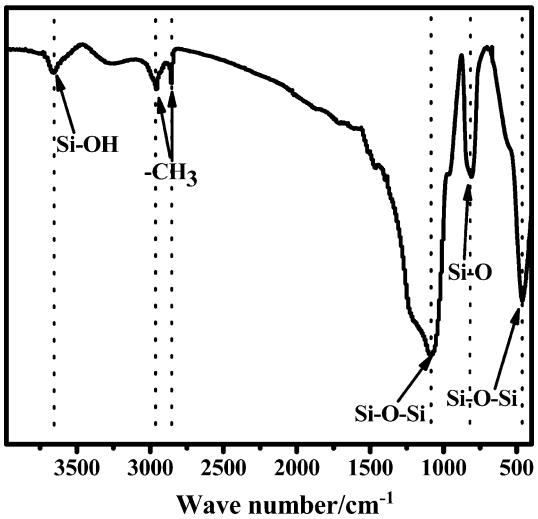

Fig. 8 FT-IR spectrum of silica aerogel microspheres (S5 sample)

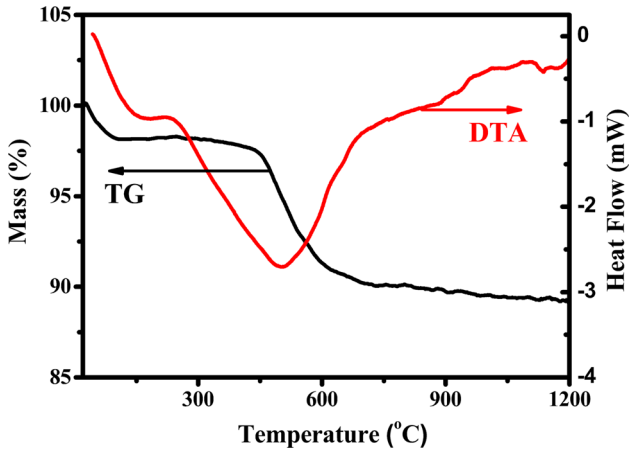

Fig. 9 TG-DTA curves of silica aerogel microspheres heated from room temperature to 1200 °C at a rate of 10 °C/min under nitrogen gas atmosphere. (S5 sample)

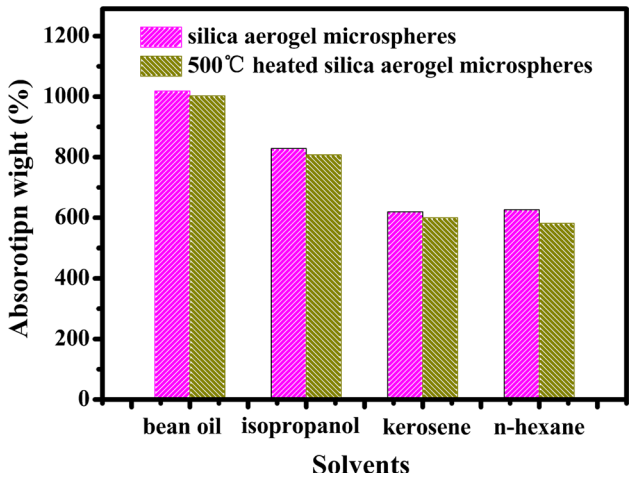

Fig. 10 The absorption ratio of silica aerogel microspheresin different solvents (S5 sample)

isopropanol, ~612 % for kerosene and ~606 % *n*-hexane, respectively. The mass of the solvent absorbed by silica aerogel microspheres depends upon the surface tension of the corresponding liquid [17]. It can be reused three times of silica aerogel microspheres for absorbing isopropanol, kerosene and *n*-hexane, except viscous bean oil. This result highlights the possibility of using silica aerogel microspheres to remove oils from water for oil spill cleanup.

4 Conclusion

We have shown that silica aerogel microspheres with a good sphericity can be formed by a two-step acid–base sol–gel reaction with emulsification technique. The smooth silica aerogel microspheres can be formed from the silica sol with the viscosity of 107 mPa s. We find that the diameter, density and roundness of the silica aerogel microspheres depend on surfactant concentrations and mechanical stirring speeds. Silica aerogel microspheres with mean diameters ranging from 40.3 to 126.1 μm, bulk densities in the range of 0.094–0.138 g/cm^3, and roundness in the range of 1.11–1.32 have been synthesized by controlling surfactant concentrations and mechanical stirring speeds. The silica aerogel microspheres show a high capacity of uptaking bean oil, isopropanol, kerosene and *n*-hexane, highlighting the possibility of using them to remove oils from water for oil spill cleanup.

Acknowledgments Financial support from the Natural Science Foundation of China (51175444), the Aviation Science Foundation of China (2013ZD68009), New Century Excellent Talents in Fujian

Province University (2013), the Natural Science Foundation of Fujian Province of China (2014J01206), and Xiamen Municipal Bureau of Science and Technology (3502Z20143009) is acknowledged.

References

1. C.J. Lee, G.S. Kim, S.H. Hyun, J. Mater. Sci. **37**, 2237–2241 (2002)
2. J.M. Schultz, K.I. Jensen, F.H. Kristiansen, Sol. Energ. Mater. Sol. C **89**, 275–285 (2005)
3. T. Herman, J. Day, J. Beamish, Phys. Rev. B **73**, 94–100 (2006)
4. A.C. Pierre, G.M. Pajonk, Chem. Rev. **102**, 4243–4265 (2002)
5. L.W. Hrubesh, J. Non-Cryst. Solids **225**, 335–342 (1998)
6. C.E. Carraher, Polym. News **30**, 386–388 (2005)
7. S. Gutzov, N. Danchova, S.I. Karakashev, M. Khristov, J. Ivanova, J. Ulbikas, J. Sol-Gel Sci. **705**, 11–516 (2014)
8. A.P. Rao, A.V. Rao, J. Mater. Sci. **45**, 51–63 (2010)
9. Z. Tan, B. Zhao, P. Shen, S. Jiang, P. Jiang, X. Wang, S. Tan, J. Mater. Sci. **46**, 7482–7488 (2011)
10. E. Baudrin, G. Sudant, D. Larcher, B. Dunn, J.M. Tarascon, Chem. Mater. **18**, 4369–4374 (2006)
11. M. Mirzaeian, P.J. Hall, Electrochim. Acta **54**, 7444–7451 (2009)
12. B. Fang, L. Binder, J. Power Sources **163**, 616–622 (2006)
13. N. Job, F. Maillard, J. Marie, S. Berthon-Fabry, J. Pirard, M. Chatenet, J. Mater. Sci. **44**, 6591–6600 (2009)
14. L. Ren, K.S. Hui, K.N. Hui, J. Mater. Chem. A **1**, 5689–5694 (2013)
15. M. Alnaief, I. Smirnova, J. Non-Cryst. Solids **356**, 1644–1649 (2010)
16. X. Wu, X. Yang, D. Wu, R. Fu, Chem. Eng. J. **138**, 47–54 (2008)
17. J.L. Gurav, A.V. Rao, D.Y. Nadargi, H. Park, J. Mater. Sci. **45**, 503–510 (2010)
18. J.G. Reynolds, P.R. Coronado, L.W. Hrubesh, Energ. Source. **23**, 831–843 (2001)
19. J.G. Reynolds, P.R. Coronado, L.W. Hrubesh, J. Non-Cryst. Solids **292**, 127–137 (2001)
20. M. Alnaief, S. Antonyuk, C.M. Hentzschel, C.S. Leopold, S. Heinrich, I. Smirnova, Micropor. Mesopor. Mater. **160**, 167–173 (2012)
21. M. Schmidt, F. Schwertfeger, J. Non-Cryst, Solids **225**, 364–368 (1998)
22. M. Alnaief, J. Smirnov, J. Supercrit. Fluids **55**, 1118–1123 (2011)
23. S.K. Hong, M.Y. Yoon, H.J. Hwang, J. Am. Ceram. Soc. **94**, 3198–3201 (2011)
24. Y.X. Yu, D.Q. Guo, A method to prepare silica aerogel microspheres, China patent, No. CN 103523789 A (2013)
25. C.A. García-González, J. Uy, M. Alnaief, I. Smirnova, Carbohyd. Polym. **88**, 1378–1386 (2012)
26. G.W. Liu, B. Zhou, A. Du, J. Shen, G.M. Wu, Colloid. Surf. A **436**, 763–774 (2013)
27. M. Alnaief, M.A. Alzaitoun, C.A. García-González, I. Smirnova, Carbohyd. Polym. **84**, 1011–1018 (2011)
28. G.H. Barth et al., *Modern methods of particle size analysis* (Wiley, New York, 1984)